

See discussions, stats, and author profiles for this publication at: <https://www.researchgate.net/publication/257434997>

Prediction of unconfined compressive strength of rock surrounding a roadway using artificial neural network

Article in *Neural Computing and Applications* · August 2012

DOI: 10.1007/s00521-012-0925-2

CITATIONS

16

READS

88

2 authors:



[Abbas Majdi](#)

University of Tehran

40 PUBLICATIONS 242 CITATIONS

[SEE PROFILE](#)



[Mohammad Rezaei](#)

University of Kurdistan

16 PUBLICATIONS 255 CITATIONS

[SEE PROFILE](#)

Prediction of unconfined compressive strength of rock surrounding a roadway using artificial neural network

Abbas Majdi · Mohammad Rezaei

Received: 23 December 2011 / Accepted: 19 March 2012 / Published online: 7 April 2012
© Springer-Verlag London Limited 2012

Abstract The unconfined compressive strength (UCS) of rocks is an important design parameter in rock engineering and geotechnics, which is required and determined for rock mechanical studies in mining and civil projects. This parameter is usually determined through a laboratory UCS test. Since the preparation of high-quality samples is difficult, expensive and time consuming for laboratory tests, development of predictive models for determining the mechanical properties of rocks seems to be essential in rock engineering. In this study, an attempt was made to develop an artificial neural network (ANN) and multivariable regression analysis (MVRA) models in order to predict UCS of rock surrounding a roadway. For this, a database of laboratory tests was prepared, which includes rock type, Schmidt hardness, density and porosity as input parameters and UCS as output parameter. To make a database (including 93 datasets), different rock samples, ranging from weak to very strong types, are used. To compare the performance of developed models, determination coefficient (R^2), variance account for (VAF), mean absolute error (E_a) and mean relative error (E_r) indices between predicted and measured values were calculated. Based on this comparison, it was concluded that performance of the ANN model is considerably better than the MVRA model. Further, a sensitivity analysis shows that rock density and Schmidt hardness were recognized as the most effective parameters, whereas porosity was

considered as the least effective input parameter on the ANN model output (UCS) in this study.

Keywords Unconfined compressive strength · Artificial neural network · Multivariable regression · Sensitivity analysis

1 Introduction

Unconfined compressive strength of rocks has an important role in design, construction, and long-term stability of surface and underground structures such as mines, tunnels, rock slopes and rock foundations. Mining engineers request the unconfined compressive strength more often than any other rock material property, that is, this parameter is essential for the stability analysis of long-wall pillars, roadways, etc. [1]. The measures and estimates of the unconfined compressive strength of rock materials is widely utilized in rock engineering, being important for rock mass classifications and rock failure criteria. This parameter is controlled by many factors such as porosity, mineralogy, density, weathering, etc. Because of this reason, some researchers proposed some empirical equations between the petrophysical parameters of the rocks and the UCS [2–6]. Generally, UCS is determined directly and indirectly by laboratory tests, as described by both the International Society for Rock Mechanics (ISRM) and the American Society for Testing Materials (ASTM) [7, 8].

Determination of the unconfined compressive strength from laboratory methods requires a large number of shaped and regular specimens and it requires carefully prepared rock samples. Also, laboratory tests present formidable problems in obtaining representative samples and long testing times. Such cores cannot always be extracted from

A. Majdi · M. Rezaei (✉)
School of Mining Engineering,
University College of Engineering,
University of Tehran,
Tehran 1439957131, Iran
e-mail: m.rezaei1360@gmail.com

weak, highly fractured, thinly bedded, foliated and block-in-matrix rocks. However, weak rocks are usually not suitable for preparing representative core samples or the preparation of such samples is boring, time consuming and expensive [9, 10]. In addition to laboratory tests, some predictive models considering simple indirect tests were developed by various investigators to predict the unconfined compressive strength [11–20]. Traditionally, statistical methods such as simple and multiple regression techniques can be employed to establish predictive models in rock engineering [21]. For example, prediction of unconfined compressive strength using statistical models has been studied by some researchers [22, 23]. In general, statistical methods based on linear regression models suffer from several demerits. As such, the statistical methods predict mean values only. Consequently, if the data extend in wide range, statistical methods cannot predict accurately. Furthermore, this method is tolerant neither to outliers nor to extreme values in the data. Moreover, it should be noted that the statistical method is not suitable to cope with nonlinear and multivariable problems [24].

The above-mentioned demerits in applying available methods of UCS prediction are in fact the main reason to adopt other alternatives to overcome these problems. Therefore, development of predictive models to determine unconfined compressive strength of rocks seems to be necessary in rock engineering. These models give viable tools to perform laboratory tests in a time and labor-efficient manner [5]. In recent years, new techniques such as artificial neural networks (ANNs) and fuzzy inference systems (FISs) have been employed for developing predictive models in complex problems. The ANN technique is considered to be one of the most appropriate tools for solving complex systems. This technique has the ability of generalizing a solution from the pattern presented to it during training process. Once the network is trained with a sufficient number of sample datasets, predictions can be done on the basis of previous learning [25]. Due to its multidisciplinary nature, ANNs are becoming popular among researchers, planners, designers, etc., as an effective tool for the success of their works. In the last two decades, an increase in artificial neural networks applications has been observed in the field of rock mechanics, geotechnics, and engineering geology [26–34]. These applications demonstrate that ANNs are efficient in solving problems in geosciences which many parameters influence the process.

In this study, an attempt has been made to develop an artificial neural network model for the prediction of unconfined compressive strength based on the information of different rock samples. For validation of the proposed ANN model, multivariable regression analysis (MVRA) was also performed on the basis of same database used in ANN modeling.

2 Artificial neural networks

Artificial neural networks (ANNs) are simplified models of the biological structure found in human brains. These models consist of elementary processing units, called neurons. It is the large amount of interconnections between these neurons and their capability to learn from data provide a strong predicting and classification tool [35]. ANNs have the potential to map complex and non-linear relations between input and output variables of a system and so they are commonly used in non-linear engineering problems. In design of engineering projects, neural network systems can be used to confirm and refine design solutions [31]. Neural networks are also able to detect similarities in inputs even though a particular input may never have been known previously. This property allows its excellent interpolation capabilities, especially when the input data are noisy. A particular network is defined using three fundamental components: transfer function, network architecture, and learning law. One has to define these constituents depending on the problem to be solved [36, 37].

2.1 Network training

A network needs first should be trained before taking new information. Although there are various algorithms for training neural networks, the feed-forward back-propagation algorithm is the most efficient one. It provides the most efficient learning procedure for multilayer neural networks. Also, the fact that back-propagation algorithms are especially capable of solving predictive problems makes them so popular. Back-propagation multilayer neural networks consist of at least three layers including input, hidden, and output layers (Fig. 1). Each layer consists of a number of elementary processing units, called neurons, and each neuron is connected to the next layer through weights, that is, neurons in the input layer will send their output as input to neurons in the hidden layer and there are similar connection between hidden and output

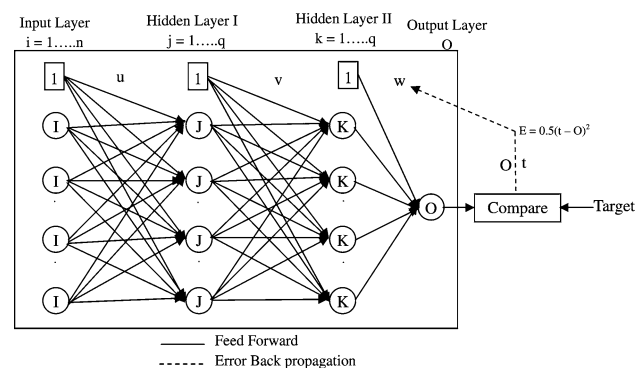


Fig. 1 Back-propagation neural network [39]

layer. The number of hidden layers and the number of respective neurons in each layer depend upon complexity of the studied problem and are achieved through trial and error method. The number of input and output neurons is the same as the number of input and output variables [33, 38].

To differentiate between the various processing units, values called biases are set up into the transfer functions. Except for the input layer, all neurons in the back-propagation network are associated with a bias neuron and a transfer function. Transfer functions are used to transform the weighted sum of all input signals to a neuron and determine the neuron output strength. The bias is much like a weight, except that it has a constant input of 1, while the transfer function sifts the summed signals received from this neuron [40]. Generally, non-linear sigmoid (LOGSIG, TANSIG) and linear (POSLIN, PURELIN) functions can be used as transfer functions. The utilization of these transfer functions depends on the purpose of the neural network. However, the sigmoid type is more efficient. The logarithmic sigmoid function (LOGSIG) is defined as [41]:

$$f = \frac{1}{(1 + e^{-e_x})} \tag{1}$$

where e_x is the weighted sum of inputs for a processing unit.

In the training process, data are processed through the input layer to hidden layer until it reaches the output layer (forward pass). In this layer, the output is compared to the actual values. The difference between both is propagated back through the network (backward pass) to update the individual weights of the connections and the biases of the individual neurons [42]. The input and output data are mainly represented as vectors called training pairs. The above process is repeated for all the training pairs in the dataset until the network error converges to a threshold defined by a corresponding function such as root mean squared error (RMSE) or summed squared error (SSE). Considering the number of neurons in the hidden layers, it can be said that insufficient neurons can cause “underfitting,” whereas excessive neurons can result in “overfitting.” In the underfitting, the requisite accuracy of the modeling is not achieved, whereas in the overfitting, the network performance would not be real because instead of realizing relationship between the patterns, network just remembers the patterns [35, 41, 43].

In Fig. 1, the j th neuron is connected with a number of inputs [26, 33]:

$$x_i = (x_1, x_2, x_3, \dots, x_n) \tag{2}$$

The net input values in the hidden layer will be calculated by the following equation

$$Net_j = \sum_{i=1}^n x_i w_{ij} + \theta_j \tag{3}$$

where x_i is the input units, w_{ij} is the weight on the connection of i th input and j th neuron, θ_j is the bias neuron and n is the number of input units.

Considering the above equation and using the convenient transfer function, that is, logarithmic sigmoid function, the net output from hidden layer is calculated as follows:

$$O_j = f(Net_j) = \frac{1}{1 + e^{-(Net_j + \theta_j)}} \tag{4}$$

The total input to the k th unit is calculated by

$$Net_k = \sum_{j=1}^n w_{jk} O_j + \theta_k \tag{5}$$

where θ_k is the bias neuron, w_{jk} is the weight between j th neuron and k th neuron.

So, the total output from k th unit will be as follows:

$$O_k = f(Net_k) \tag{6}$$

During the learning process, the network is presented with a pair of patterns, an input pattern and a corresponding output pattern. The network computes its own output pattern using its weights and thresholds. Now, the actual output is compared with the desired output. Hence, the error for any output in layer k is calculated by this equation:

$$e_t = t_k - O_k \tag{7}$$

where t_k and O_k are the desired output and actual output, respectively.

The total error function is acquired by following equation:

$$E = 0.5 \sum_{k=1}^n (t_k - O_k)^2 \tag{8}$$

Training of the network is basically a process of arriving at an optimum weight space for the network. The steepest descent error surface is made using the following rule:

$$\nabla W_{jk} = -\eta \frac{\delta E}{\delta W_{jk}} \tag{9}$$

where η and E are the learning rate parameter and error function, respectively.

The update of weights for the $(n + 1)$ th pattern is given as follows:

$$W_{jk}(n + 1) = W_{jk}(n) + \nabla W_{jk}(n) \tag{10}$$

Similar logic applies to the connections between the hidden and output layers. This procedure is repeated with each pair of training case. Each pass through all the

training patterns is called a cycle or epoch. The process is then repeated as many epochs as needed until the error is within the user-specified goal [33].

3 Data collection and preparation

Data collection is one of the most important stages in the ANN modeling. Here, rock samples were prepared for unconfined compressive strength tests from different coalfields, in which the parameters such as rock type, Schmidt hardness, density and porosity were also measured. For this, the core specimens of different rock types with NX-size (54 mm), right cylinder shape and a height-to-diameter ratio of 2.5:1 in accordance with the procedure suggested by ISRM were selected. Besides the measured Schmidt hardness, density, porosity and unconfined compressive strength values, a description of the rock type is given for the individual rock samples in the dataset. However, to make use of the linguistic descriptions in ANN and MVRA, those descriptions have to be converted into numerical values. It is important to be consistent in such a conversion. Thus, the rock type is classified according to its strength (Table 1).

In this study, 93 datasets were prepared and divided into training and testing datasets using sorting method to maintain statistical consistency. Among the total datasets, 20 % were chosen for testing and validation of the model. Table 2 indicates statics of relevant parameters as well as their respective symbols. Also, a list of sample data used for training the ANN model and constructing the MVRA model is given in Table 3.

4 Determination of optimum network

To make an optimum architecture of ANN model, different types of networks must be examined based on trial and error method. For this, root mean square error (RMSE) is calculated for all the models, and accordingly, the model with minimum RMSE is chosen as the optimum model. The optimum number of neurons in hidden layers is also obtained by trial and error method based on the minimum RMSE. Figure 2 shows the network performance for different numbers of neuron in hidden layers. In this figure, networks with different number of neurons in hidden layers were examined to determine the optimum number of hidden neuron. These neurons can be located in one or two hidden layers that their arrangements will be determined in the next step. As can be seen from this figure, a network with 17 neurons in hidden layers has the best performance compared with the others. Based on the optimum number of neurons in hidden layers, RMSE was calculated for

Table 1 Conversion values of the rock types

Rock type	Mean UCS (MPa)	Numeric value
Diabase	303.18	1
Gabbro	285.5	2
Olivine	280	3
Amphibolite	280	3
Dolerite	275	4
Granodiorite	275	4
Eclogite	270	5
Serpentine	263.97	6
Dunite	260	7
Norite	260	7
Quartzite	257.87	8
Quartz diorite	250	9
Groana	250	9
Peridotite	250	9
Pyroxenite	245	10
Basalt	231	11
Diopside	230	12
Granite	224.53	13
Syenite	218	14
Rhyolite	200	15
Anorthosite	200	15
Gneiss	174.4	16
Slate	170	17
Anhydride	150	18
Dolomite	143	19
Marble	135.2	20
Siltstone	131.49	21
Limestone	116.84	22
Sandstone	104.99	23
Tuff	97	24
Pitchstone	90	25
Shale	85	26
Marl	85	26
Gypsum	75.3	27
Chalk	61.66	28
Conglomerate	38	29
Schist	33.6	30

different types of the models including one and two hidden layers with different number of neurons and transfer functions (Table 4). RMSE is calculated by this equation [44]:

$$\text{RMSE} = \sqrt{\frac{1}{n} \sum_{i=1}^n (A_{i\text{meas}} - A_{i\text{pred}})^2} \quad (11)$$

where $A_{i\text{meas}}$, $A_{i\text{pred}}$ and n are the i th measured element, i th predicted element and the number of datasets, respectively.

Table 2 Description of input and output parameters in the modeling

Type of data	Parameter	Symbol	Max	Min	SD	Variance
Input	Rock type (-)	<i>R</i>	30	1	7.84	61.6
	Schmidt hardness (-)	SH	71.33	25.25	8.58	73.65
	Density (g/cm ³)	<i>D</i>	3.8	1.65	0.43	0.19
	Porosity (%)	<i>P</i>	41.17	0.1	7.8	60.88
Output	Unconfined compressive strength (MPa)	UCS	361.37	23	84.09	7072.73

Table 3 Sample of dataset used for modeling

No.	<i>R</i> (-)	SH (-)	<i>D</i> (g/cm ³)	<i>P</i> (%)	UCS (MPa)
1	Sandstone	61	2.6	3.56	184
2	Limestone	54	2.56	7.7	127
3	Eclogite	55	3.4	3	260
4	Schist	2.6	30	42.16	33.6
5	Dolomite	50.5	2.67	2.17	110
6	Pyroxenite	55.16	3.24	3.7	230
7	Pitchstone	51	2.33	9.6	90
8	Diabase	2.95	0.17	65.5	361.37
9	Gypsum	48.33	2.2	14.32	70
10	Anhydride	41.66	3.8	6	150

Table 4 Results of some models with different architecture and transfer functions

No.	Network architecture	Transfer function	RMSE
1	4-17-1	POSLIN	0.0121
2	4-17-1	PURELIN	0.0267
3	4-10-7-1	TANSIG	0.0098
4	4-7-10-1	LOGSIG	0.0086
5	4-11-6-1	PURELIN	0.0078
6	4-6-11-1	POSLIN	0.0082
7	4-5-12-1	TANSIG	0.0076
8	4-5-12-1	LOGSIG	0.0064
9	4-9-8-1	TANSIG	0.0058
10	4-9-8-1	LOGSIG	0.0043

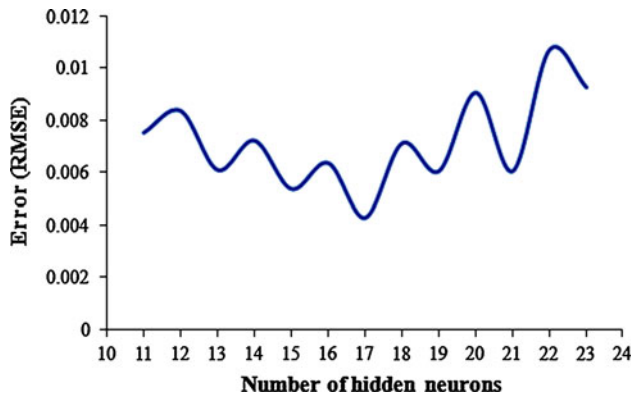


Fig. 2 Network performances for different numbers of neuron in hidden layers

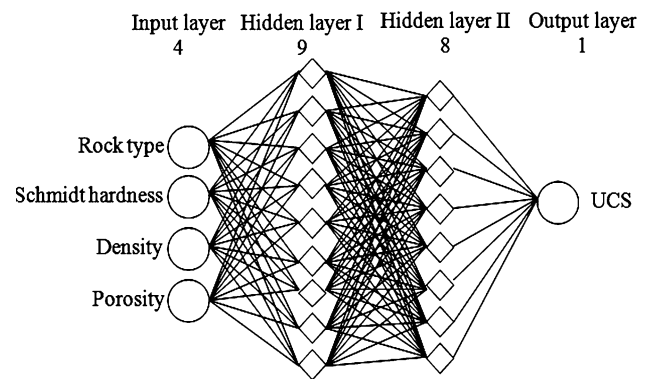


Fig. 3 Suggested MNN for the UCS prediction

As can be seen from Fig. 2 and Table 4, the network with architecture 4-9-8-1 and LOGSIG transfer function has the minimum RMSE, hence considered as the optimum model. Figure 3 shows a graphical presentation of this network. Also, the whole information of optimum network architecture is given in Table 5.

To test and validate the optimum ANN model, about 20 % of dataset was chosen randomly. These data were not used in training the network. It validates the ANN application in a more versatile way. The results of the network are presented in this section to demonstrate its performance. Correlation coefficient between the predicted and

measured values of UCS is taken as the network performance. The prediction was based on the input datasets that discussed in the previous section. Figure 4 shows the optimum network results in terms of correlation coefficient for training, validation, and testing processes.

5 Multivariable regression analysis

Multivariable regression analysis (MVRA) is an extension of the regression analysis that includes additional independent variables in the predictive equation. This method

Table 5 Whole information of optimum network architecture

Number of input neurons	1
Number of hidden layers	2
Number of hidden neurons	17
Number of output neurons	1
Number of training epochs	300
Number of training datasets	75
Number of testing datasets	18
Training function	Levenberg–Marquardt back-propagation
Transfer function	LOGSIG
Learning rate	0.1
Error goal	0

is employed to establish a mathematical formula in order to predict the dependent variables based on the known independent variables [45]. Here, a relationship between unconfined compressive strength (output) and the other relevant parameters (inputs), that is, Schmidt hardness, density, and porosity, has been discussed based on the multivariable regression. To generate multivariate relation on the basis of same database as considered for training the ANN model, the statistical software package SPSS19 was used. Accordingly, this equation is obtained for the prediction of UCS:

$$UCS = -229 + 3.74SH + 76.2D - 3.24P \tag{12}$$

6 Comparison of models performance

To control the prediction performances of both the ANN and MVRA models, their predicted UCS are compared with the measured ones. For this purpose, four key performance indices (KPIs), including determination coefficient (R^2), variant account for (VAF), mean absolute error (E_a), and mean relative error (E_r) were chosen and calculated based on the testing data. Further, these indices are computed using the following equations [35, 44].

$$VAF = 100 \left(1 - \frac{\text{var}(A_{imeas} - A_{ipred})}{\text{var}(A_{ipred})} \right) \tag{13}$$

$$E_a = |A_{imeas} - A_{ipred}| \tag{14}$$

$$E_r = \left(\frac{|A_{imeas} - A_{ipred}|}{A_{imeas}} \right) \times 100 \tag{15}$$

where, A_{imeas} is the i th measured element, A_{ipred} is the i th predicted element.

For testing the models, 18 datasets that were not incorporated into the development of the models were used. Based on the testing data, the models performance indices were calculated and summarized in Table 6. Also,

Fig. 4 Results of the optimum neural network model

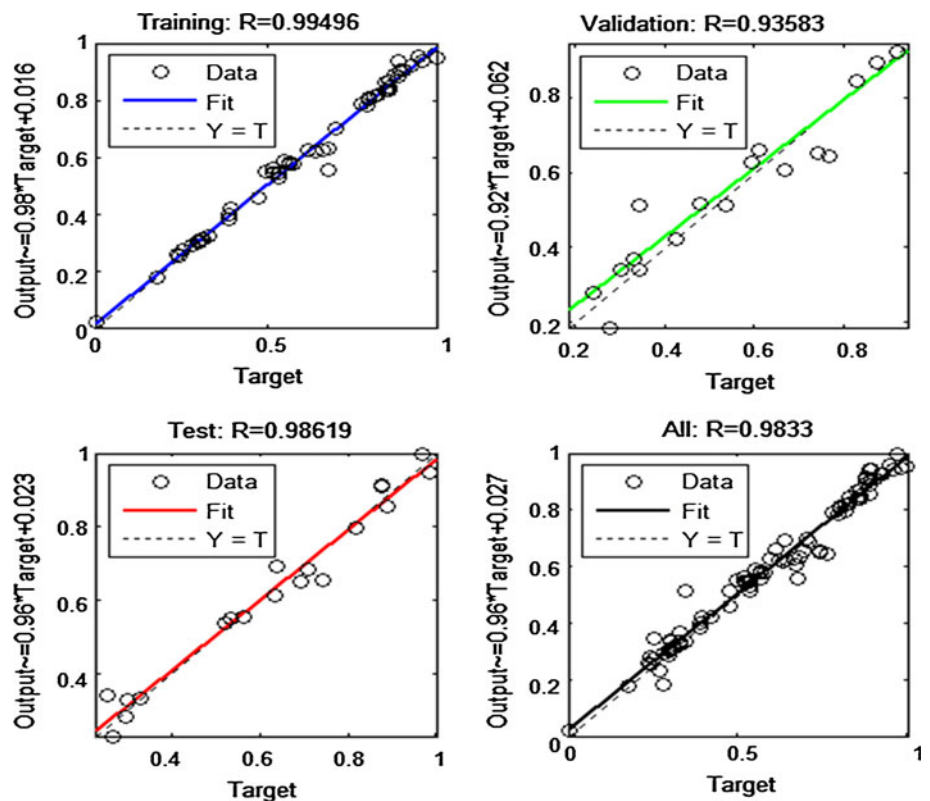


Table 6 Performance indices of the models

Index	ANN model	MVRA model
R^2	97.25 %	89.88 %
VAF	95.65 %	91.61 %
E_a	0.0942	0.1117
E_r	1.1127 %	2.3422 %

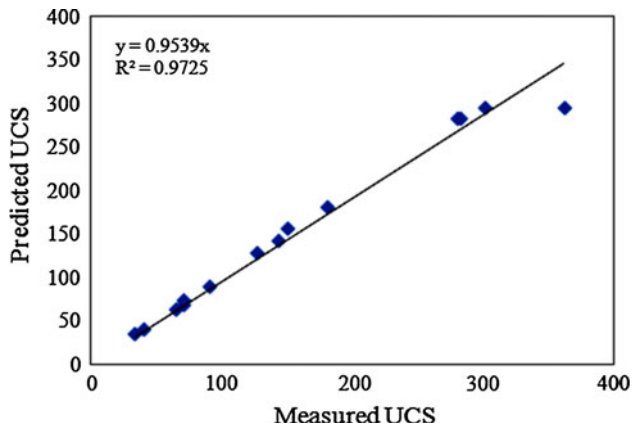


Fig. 5 Comparison between the measured and predicted UCS for the ANN model

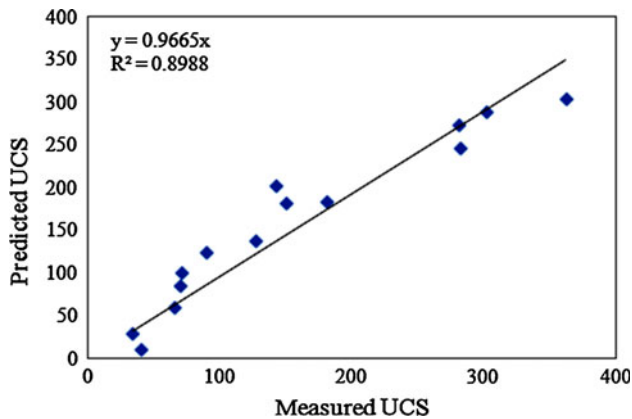


Fig. 6 Comparison between measured and predicted UCS for the MVRA model

comparison between predicted and measured UCS for ANN and MVRA models are shown in the Figs. 5 and 6, respectively. It can be seen from the above comparisons that the performance of ANN model in terms of those indices is much better than MVRA model and its results are closer to the real values.

7 Sensitivity analysis

A sensitivity analysis was used to identify the significance of each input parameter on the objective (output) parameter

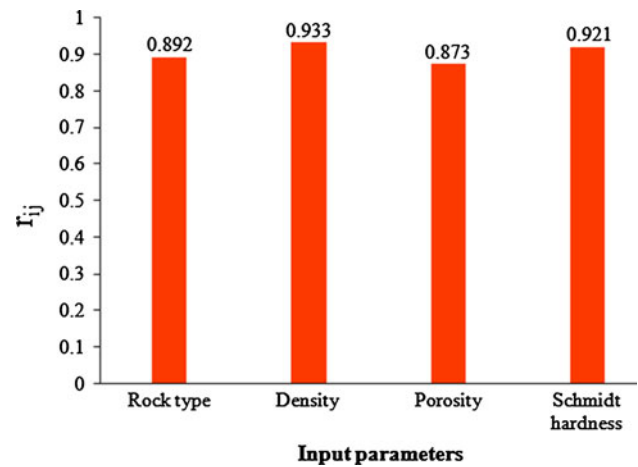


Fig. 7 Strengths of relation (r_{ij}) between the UCS and input parameters

in the modeling. The Cosine Amplitude Method (CAM) is one of the sensitivity analysis methods that used to obtain the express similarity relations between the related parameters [46]. To apply this method, all of the data pairs were expressed in common X-space. The data pairs used to construct a data array X defined as:

$$X = \{X_1, X_2, X_3, \dots, X_m\} \tag{16}$$

Each of the elements, X_i , in the data array X is a vector of lengths of m , that is:

$$X_i = \{x_{i1}, x_{i2}, x_{i3}, \dots, x_{im}\}_1 \tag{17}$$

Thus, each of the data pairs can be thought of as a point in m -dimensional space, where each point requires m -coordinates for a full description. Each element of a relation, r_{ij} , results in a pairwise comparison of two data pairs. Therefore, the strength of the relation between the data pairs, x_i and x_j , is given by this equation:

$$r_{ij} = \frac{\sum_{k=1}^m x_{ik}x_{jk}}{\sqrt{\sum_{k=1}^m x_{ik}^2 \sum_{k=1}^m x_{jk}^2}} \tag{18}$$

Here, the strengths of relations (r_{ij} values) between the UCS (output) and input parameters using the CAM method are shown in Fig. 7. As can be seen, the most effective parameter on the UCS is density and Schmidt hardness, whereas porosity is the least effective parameter on the UCS.

8 Conclusion

In this study, a neural network model was developed to predict unconfined compressive strength. A feed-forward back-propagation neural network with architecture 4-9-8-1 and RMSE of 0.0043 was found to be an optimum network. To approve the capability of this approach, the obtained

results are compared with the results of MVRA model on the basis of same data. Performance of the models has been evaluated by calculating determination coefficient (R^2), variance account for (VAF), mean absolute error (E_a), and mean relative error (E_r). For the ANN model, R^2 , VAF, E_a , and E_r were calculated 97.25, 95.65 %, 0.0942 MPa, 1.1127 %, respectively, whereas for the MVRA model, R^2 , VAF, E_a , and E_r were determined 89.88 %, 91.61 %, 0.1117 MPa, 2.3422 %, respectively. It was concluded that the ANN results indicate very close agreement for the UCS with the laboratory datasets as compared with the MVRA predictions. Moreover, sensitivity analysis of the ANN results revealed that the most effective parameters on the UCS are the density and Schmidt hardness, whereas porosity is the least effective parameter on the UCS in this study. Considering the above results, it can be concluded that the ANN model has good capability in predicting UCS and proves to be simpler and more economical in comparison with tedious and expensive laboratory procedures. Therefore, this technique can be used to determine unconfined compressive strength in mining application such as failure analysis of long walls, stability analysis of pillars, roadways, etc.

References

- Bieniawski ZT (1974) Estimating the strength of rock materials. *J S Afr Inst Min Metall* 74:312–320
- Onodera TF, Yoshinaka R, Oda M (1974) Weathering and its relation to mechanical properties of granite. In: *Proceedings of the 3rd congress of ISRM, vol II(A), Denver, USA*, pp 71–78
- Fahy MP, Guccione MJ (1979) Estimating strength of sandstones using petrographic thin-section data. *Bull Assoc Eng Geol* 16(4):467–485
- Prikryl R (2001) Some microstructural aspects of strength variation in rocks. *Int J Rock Mech Min Sci* 38:671–682
- Zorlu K, Gokceoglu C, Ocakoglu F, Nefeslioglu HA, Acikalin S (2008) Prediction of uniaxial compressive strength of sandstones using petrography-based models. *Eng Geol* 96:141–158
- Cevik A, Sezer EA, Cabalar AF, Gokceoglu C (2011) Modeling of the uniaxial compressive strength of some clay-bearing rocks using neural network. *Appl Soft Comput* 11:2587–2594
- ISRM (1985) Suggested method for determining point load strength. *Int J Rock Mech Min Sci Geomech Abstr* 22:51–60
- ASTM (1986) Standard test method of unconfined compressive strength of intact rock core specimens. D2938
- Alber M, Kahraman S (2009) Predicting the uniaxial compressive strength and elastic modulus of a fault breccia from texture coefficient. *Rock Mech Rock Engng* 42:117–127
- Kayabali K, Selcuk L (2010) Nail penetration test for determining the uniaxial compressive strength of rock. *Int J Rock Mech Min Sci* 47:265–271
- Kahraman S (2001) Evaluation of simple methods for assessing the uniaxial compressive strength of rock. *Int J Rock Mech Min Sci* 38(7):981–994
- Shakoor A, Bonelli RE (1991) Relationship between petrographic characteristics, engineering index properties and mechanical properties of selected sandstone. *Bull Assoc Eng Geol* 28(1): 55–71
- Tsiambaos G, Sabatakakis N (2004) Considerations on strength of intact sedimentary rocks. *Eng Geol* 72:261–273
- Chau KT, Wong RHC (1996) Uniaxial compressive strength and point load strength. *Int J Rock Mech Min Sci Geomech Abstr* 33:183–188
- Yilmaz I, Sendir H (2002) Correlation of Schmidt hardness with unconfined compressive strength and young modulus in gypsum from Sivas (Turkey). *Eng Geol* 66:211–219
- Fener M, Kahraman S, Bilgil A, Gunaydin O (2005) A comparative evaluation of indirect methods to estimate the compressive strength of rocks. *Rock Mech Rock Engng* 38(4):329–334
- Sonmez H, Tuncay E, Gokceoglu C (2004) Models to predict the uniaxial compressive strength and the modulus of elasticity for Ankara Agglomerate. *Int J Rock Mech Min Sci* 41(5):717–729
- Sonmez H, Gokceoglu C, Medley EW, Tuncay E, Nefeslioglu HA (2006) Estimating the uniaxial compressive strength of a volcanic bimrock. *Int J Rock Mech Min Sci* 43(4):554–561
- Heidari M, Khanlari GR, Torabi Kaveh M, Kargarian S (2011) Predicting the uniaxial compressive and tensile strengths of gypsum rock by point load testing. *Rock Mech Rock Eng*. doi:10.1007/s00603-011-0196-8
- Yasar E, Erdogan Y (2004) Correlating sound velocity with the density, compressive strength and Young's modulus of carbonate rocks. *Int J Rock Mech Min Sci* 41(5):871–875
- Dehghan S, Sattari Gh, Chehreh Chelgani S, Aliabadi MA (2010) Prediction of uniaxial compressive strength and modulus of elasticity for Travertine samples using regression and artificial neural networks. *Mini Sci Technol* 20(1):0041–0046
- Verwaal W, Mulder A (1993) Estimating rock strength with the Equotip hardness tester. *Int J Rock Mech Min Sci Geomech Abstr* 30(6):659–662
- Asef MR (1995) Equotip as an index test for rock strength properties. M.Sc. thesis, ITC Delft
- Alvarez Grima M, Babuska R (1999) Fuzzy model for the prediction of unconfined compressive strength of rock samples. *Int J Rock Mech Min Sci* 36:339–349
- Khandelwal M, Roy MP, Singh PK (2004) Application of artificial neural network in mining industry. *Ind Min Eng J* 43:19–23
- Singh VK, Singh D, Singh TN (2001) Prediction of strength properties of some schistose rocks from petrographic properties using artificial neural networks. *Int J Rock Mech Min Sci* 38(2):269–284
- Yilmaz I, Yuksek AG (2008) An example of artificial neural network (ANN) application for indirect estimation of rock parameters. *Rock Mech Rock Eng* 41(5):781–795
- Tiryaki B (2008) Predicting intact rock strength for mechanical excavation using multivariate statistics, artificial neural networks and regression trees. *Eng Geol* 99:51–60
- Ali M, Chawathe A (2000) Using artificial intelligence to predict permeability from petrographic data. *Comput Geosci* 26:915–925
- Ranjith PG, Khandelwal M (2011) Artificial neural network for prediction of air flow in a single rock joint. *Neural Comput Appl*. doi:10.1007/s00521-011-0595-5
- Mert E, Yilmaz S, Inal M (2011) An assessment of total RMR classification system using unified simulation model based on artificial neural networks. *Neural Comput Appl* 20:603–610
- Çanakçı H, Baykasoğlu A, Güllü H (2009) Prediction of compressive and tensile strength of Gaziantep basalts via neural networks and gene expression programming. *Neural Comput Appl* 18:1031–1041
- Bhatnagar A, Khandelwal M (2011) An intelligent approach to evaluate drilling performance. *Neural Comput Appl*. doi:10.1007/s00521-010-0457-6

34. Amini H, Gholami R, Monjezi M, Torabi SR, Zadhesh J (2011) Evaluation of fly rock phenomenon due to blasting operation by support vector machine. *Neural Comput Appl*. doi:[10.1007/s00521-011-0631-5](https://doi.org/10.1007/s00521-011-0631-5)
35. Rezaei M, Monjezi M, Ghorbani Moghaddam S, Farzaneh F (2011) Burden prediction in blasting operation using rock geomechanical properties. *Arab J Geosci*. doi:[10.1007/s12517-010-0269-0](https://doi.org/10.1007/s12517-010-0269-0)
36. Simpson PK (1990) Artificial neural system-foundation, paradigm, application and implementations. Pergamon Press, New York
37. Kosko B (1994) Neural networks and fuzzy systems: a dynamical systems approach to machine intelligence. Prentice Hall, New Delhi
38. Khandelwal M, Kumar DL, Mohan Y (2011) Application of soft computing to predict blast-induced ground vibration, *Engineering with computers*. *Eng Comput* 27:117–125
39. Neaupane KM, Achet SH (2004) Use of back propagation neural network for landslide monitoring: a case study in the higher Himalaya. *Eng Geol* 74:213–226
40. Basheer IA, Hajmeer M (2000) Artificial neural networks: fundamentals, computing, design, and application. *J Microbiol Method* 43:3–31
41. Demuth H, Beal M, Hagan M (1996) Neural network tool box 5 user's guide. The Math Work, Natick
42. Khandelwal M, Singh TN (2006) Prediction of blast induced ground vibrations and frequency in opencast mine-a neural network approach. *J Sound Vibrat* 289:711–725
43. Haykin S (1999) Neural networks, a comprehensive foundation, USA, 2nd edn. Prentice Hall, USA
44. Tzamos S, Sofianos AI (2006) Extending the Q system's prediction of support in tunnels employing fuzzy logic and extra parameters. *Int J Rock Mech Min Sci* 43:938–949
45. Jennrich RI (1995) An Introduction to computational statistics-regression analysis. Prentice Hall, Englewood Cliffs, NJ
46. Jong YH, Lee CI (2004) Influence of geological conditions on the powder factor for tunnel blasting. *Int J Rock Mech Min Sci* 41(Supplement 1):533–538